Acta Mechanica Sinica (2012) 28(4):1058–1067
DOI 10.1007/s10409-012-0122-7

RESEARCH PAPER

The effect of large deformation and material nonlinearity on gel indentation

Zheng Duan · Yonghao An · Jiaping Zhang · Hanqing Jiang

Received: 4 May 2012 / Revised: 12 June 2012 / Accepted: 5 July 2012

Abstract A gel, an aggregate of polymers with solvents, has dual attributes of solid and liquid as solvent migrates in and out of the polymer network. Indentation has recently been used to characterize the mechanical properties of gels. This paper evaluates the effects of large deformation and material nonlinearity on gel indentation through theoretical modeling and finite element analysis. It is found that large deformation significantly affects the interpretation of the experimental observations and the classical relation between indentation force and depth has limitations for large deformation. The material nonlinearity does not play a very important role on indentation experiment so that the poroelasticity is a good approximation. Based on these observations, this paper proposes an alternative approach to measure the mechanical properties of gels, namely, uniaxial compression experiment.

Keywords Gel indentation · Large deformation · Finite element simulation

1 Introduction

A gel is the aggregated solvent and crosslinked polymeric network. As the solvent migrates in and out the network, gel swells and shrinks, respectively, which endows gels the capability of large and reversible deformation. The gels have found diversified applications in nature and engineering due to the dual attributes of solids and liquids, such as drug delivery [1, 2], tissue engineering [3, 4], food processing [5], and oil field management [6, 7]. It is then important to obtain the mechanical properties of gels for abovementioned applications. Recently, indentation experiment that has been successfully used to probe hard materials (e.g., metals and ceramics) is adopted as a method to characterizes gels and soft materials [8–11]. To measure the time-dependent material behavior due to the migration of solvent in and out the network of gels, the creep experiments (i.e., indentation with a constant force) and relaxation experiments (i.e., indentation with a fixed depth) can be conducted. Specifically for a relaxation indentation experiment, the gel is suddenly indented by a fixed indentation depth and the applied force gradually relaxes as the solvent migrates out of the gel network. To interpret the indentation experiments, the finite element modeling has been conducted correspondingly [12–16]. The shear modulus, Poisson's ratio and diffusivity of solvent into the network can be calculated.

In these theoretical efforts, gel is modeled as a poroelastic media [17]. Based on the Boussinesq solution, the relationship between the force applied on indenter, deformation of the gel and the material properties of gel is established and used to extract the material properties of gels [12–16, 18]. For instance, force F is applied to indent a depth h using a spherical indenter with radius R, forming a contact radius a, as shown in Fig. 1. For $a \ll R$, the contact radius and the applied force F are given by [18]

$$a = \sqrt{Rh}, \tag{1}$$

$$F = \frac{8Gha}{3(1-\nu)}, \tag{2}$$

where G is shear modulus, ν is Poisson's ratio. For given indentation depth h and indenter radius R, the material properties can be calculated based on the applied force F. This equation is the foundation of indentation experiment for hard materials and has been adopted for soft materials as well. A noticeable difference between indenting hard and soft materials is the range of deformation. For hard materials with modulus on the order of 100 GPa, the deformation is typically very small with strain on the order of few percent. However for soft materials (e.g., gels) with modulus on the order of 1 MPa or even smaller, large deformation (on the order of tens of percent) can be easily achieved. Therefore, it is thus important to examine if the force-indentation depth relationship (e.g., Eq. (2)) is valid for large deformation.

Z. Duan · Y. An · J. Zhang · H. Jiang (✉)
School for Engineering of Matter,
Transport and Energy, Arizona State University,
Tempe, AZ 85287, USA
e-mail: hanqing.jiang@asu.edu

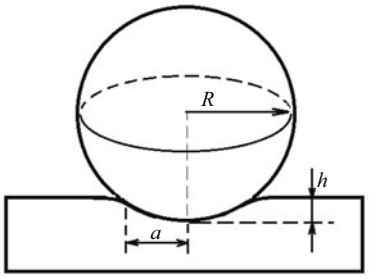

Fig. 1 Schematic of a spherical indenter with radius R on an indented material. h is the indentation depth and a is the contact radius

As a simple examination, we conducted finite element analysis using commercial package ABAQUS by indenting a relatively hard material with elastic modulus of 1 GPa and Poisson's ratio of 0.3 by a rigid spherical indenter with radius of $R = 3$ mm. The contact between the rigid indenter and the hard material is considered frictionless. 12 395 three-dimensional brick elements (C3D8) have been used in the finite element analysis and finer meshes (approximately 400 elements) are used for the region right underneath the indenter. Mesh refinement is reached for convergent results. Figure 2a compares the indentation force F obtained from finite element analysis and Eq. (2) versus the indentation depth h. It is observed that the results from finite element analysis and Eq. (2) are consistent as the indentation depth h is less than 0.02 mm but start to deviate significantly beyond this indentation depth. Figures 2b and 2c provide the contour plots of the logarithmic strain in the vertical direction for two indentation depths, namely $h = 0.02$ mm (Fig. 2b) and $h = 0.1$ mm (Fig. 2c). It is found that the absolute value of the maximal strain for $h = 0.02$ mm is around 2%, which is still within the range of small deformation. However, the strain increases to about 10% for $h = 0.1$ mm, which is clearly large deformation. This examination shows that large deformation plays an important role on indentation experiments. At the range of large deformation, the simple relationship between applied force F and indentation depth h (e.g., Eq. (2)) does not hold anymore. In fact, this discrepancy has been noticed and some empirical correction functions have been applied for deeper indentation [14]. As the large deformation is always the case for gel indentation, the effect of large deformation on gel indentation needs to be evaluated.

Aforementioned theoretical work on gel indentation modeled the gel as poroelastic material. Specifically, the stress σ_{ij} of a gel linearly depends on strain $\varepsilon_{ij} = (u_{i,j} + u_{j,i})/2$ and the chemical potential μ of the solvent in the gel,

$$\sigma_{ij} = 2G\left(\varepsilon_{ij} + \frac{\nu\varepsilon_{kk}\delta_{ij}}{1-2\nu}\right) - \frac{\mu\delta_{ij}}{v}, \tag{3}$$

where v is the specific volume of the solvent molecule. The last term on poroelasticity represents the hydrostatic pressure caused by the change of the chemical potential of the solvent, or equivalently the migration of the solvent. This constitutive relation is linear. However, it has been showed that as the solvent migrates in and out of the gel, the stress–strain relation can be highly nonlinear [19]. Thus the material nonlinearity may also play a role on gel indentation.

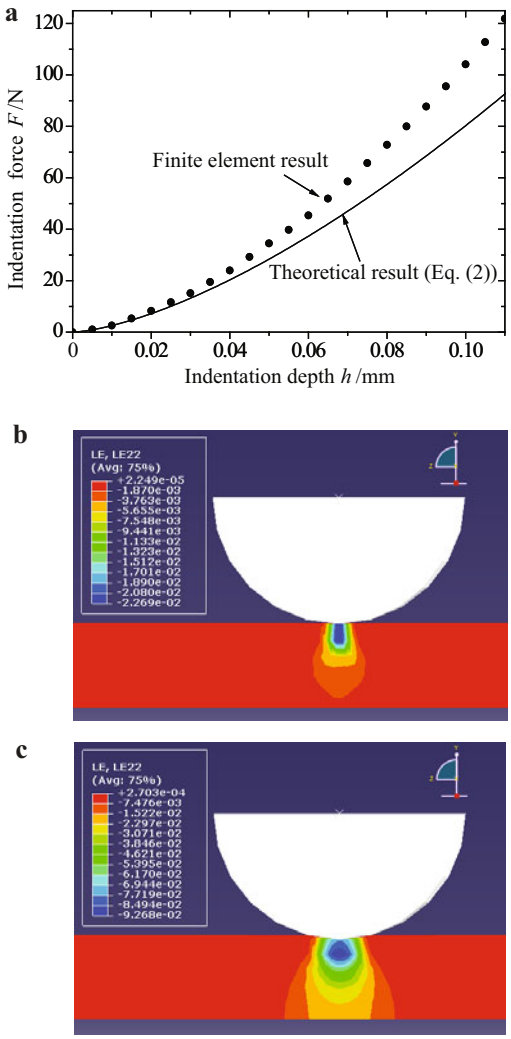

Fig. 2 Indenting a hard material with Young's Modulus 1 GPa, Poisson's ratio 0.3 by a rigid spherical indenter with radius of 3 mm. **a** Indentation force F versus indentation depth h for both finite element result and theoretical result (Eq. (2)); **b** Strain contour for shallow indentation depth $h = 0.02$ mm. **c** Strain contour for deep indentation depth $h = 0.1$ mm

In this paper, we have evaluated the effects of large deformation and material nonlinearity on gel indentation and suggested a means to more accurately and easily probe the mechanical properties of gel. Since the poroelasticity model has been widely used to study the gel indentation [11, 20, 21], we start from the linearization of nonlinear

gel constitutive relation and then evaluate the linearized constitutive relations in Sect. 2. In Sect. 3, finite element analysis has been conducted to study the short-time and long-time limits of gel indentation upon sudden application of a force. The focus is on the applicability of the simple force-deformation (e.g., Eq. (2)) for gel indentation when large deformation and material nonlinearity come into play. In Sect. 4, we presented a simpler experiment and analysis that can characterize the mechanical properties of gels even under large deformation.

2 Evaluation of the linearized gel constitutive relation

In this section, we evaluated the applicability of the linearized constitutive relation (e.g., Eq. (3) for poroelasticity) on large deformation. This evaluation is based on the comparison of a nonlinear gel constitutive relation and its linearization that takes the similar functional expression as Eq. (3). We adopt the nonlinear constitutive relation from a coupled diffusion and large deformation theory for polymeric gels [19].

Let λ_1, λ_2, and λ_3 be the three stretches along the principal directions (e.g., N_1, N_2, N_3) due to swelling. The true stresses in the principal directions are given by

$$\begin{aligned}
\sigma_1 &= \frac{NkT}{\lambda_2\lambda_3}\left(\lambda_1 - \frac{1}{\lambda_1}\right) - \left\{\frac{\mu}{v} - \frac{kT}{v}\left[\log\left(1 - \frac{1}{\lambda_1\lambda_2\lambda_3}\right) + \frac{1}{\lambda_1\lambda_2\lambda_3} + \frac{\chi}{\lambda_1^2\lambda_2^2\lambda_3^2}\right]\right\} \\
\sigma_2 &= \frac{NkT}{\lambda_1\lambda_3}\left(\lambda_2 - \frac{1}{\lambda_2}\right) - \left\{\frac{\mu}{v} - \frac{kT}{v}\left[\log\left(1 - \frac{1}{\lambda_1\lambda_2\lambda_3}\right) + \frac{1}{\lambda_1\lambda_2\lambda_3} + \frac{\chi}{\lambda_1^2\lambda_2^2\lambda_3^2}\right]\right\} \\
\sigma_3 &= \frac{NkT}{\lambda_1\lambda_2}\left(\lambda_3 - \frac{1}{\lambda_3}\right) - \left\{\frac{\mu}{v} - \frac{kT}{v}\left[\log\left(1 - \frac{1}{\lambda_1\lambda_2\lambda_3}\right) + \frac{1}{\lambda_1\lambda_2\lambda_3} + \frac{\chi}{\lambda_1^2\lambda_2^2\lambda_3^2}\right]\right\}
\end{aligned}, \tag{4}$$

where N is the number of polymer chains in the gel per unit volume of the dry polymers, kT is the temperature in the unit of energy, χ is a dimensionless parameter characterizing the polymer-solvent interaction. In fact, NkT is the shear modulus of the polymer at the dry state under the small strain condition. The last term in Eq. (4)

$$\frac{\mu}{v} - \frac{kT}{v}\left[\log(1 - \frac{1}{\lambda_1\lambda_2\lambda_3}) + \frac{1}{\lambda_1\lambda_2\lambda_3} + \frac{\chi}{\lambda_1^2\lambda_2^2\lambda_3^2}\right] \tag{5}$$

is the osmotic pressure caused by the migration of the solvent in and out the polymer network. Here both the polymer network and solvent molecular are considered incompressible. In other words, the migration of the solvent in and out the polymer network is the sole cause of the volume change of the gel.

As the gel reaches equilibrium under no constraint and external forces, the chemical potential of the solvent inside the gel balances with that of the external solvent and the gel swells freely, characterized by vanishing chemical potential $\mu = 0$, vanishing stress $\sigma_1 = \sigma_2 = \sigma_3 = 0$ and isotropic swelling $\lambda_1 = \lambda_2 = \lambda_3 = \lambda_{eq}$. The equilibrium swelling ratio λ_{eq} can be determined by solving Eq. (4). In gel indentation experiment, the fully swollen gel is indented. In the following, we will examine the linearization of a fully swollen gel.

A fully swollen gel is subjected to an uniaxial stress, for example, along N_1-direction. Two distinct states are discussed separately:

(1) Short-time limit: unrelaxed state

Right after the uniaxial stress is imposed on a fully swollen gel, at time $t = 0^+$, the solvent molecules have no time to migrate out of the fully swollen gel and the gel behaves as an incompressible material, i.e.,

$$\lambda_1\lambda_2\lambda_3 = \lambda_{eq}^3. \tag{6}$$

Denote the nominal strain in N_1-direction as ε, given by

$$\lambda_1 = \lambda_{eq}(1 + \varepsilon). \tag{7}$$

Here the fully swollen state has been used as the reference state for the uniaxial stress state. Thus the incompressibility condition for the short-limit (i.e., Eq. (6)) gives the stretch in the lateral directions (i.e., N_2 and N_3),

$$\lambda_2 = \lambda_3 = \sqrt{\frac{\lambda_{eq}^2}{(1 + \varepsilon)}}. \tag{8}$$

Substitute Eqs. (7) and (8) into Eq. (4), the true stresses become

$$\begin{aligned}
\sigma_1 &= NkT\frac{1 + \varepsilon}{\lambda_{eq}^2}\left[\lambda_{eq}(1 + \varepsilon) - \frac{1}{\lambda_{eq}(1 + \varepsilon)}\right] + \frac{kT}{v}\left[\log\left(1 - \frac{1}{\lambda_{eq}^3}\right) + \frac{1}{\lambda_{eq}^3} + \frac{\chi}{\lambda_{eq}^6}\right] - \frac{\mu}{v}, \qquad (9) \\
\sigma_2 &= \sigma_3 = \frac{NkT}{\lambda_{eq}^2\sqrt{1 + \varepsilon}}\left(\frac{\lambda_{eq}}{\sqrt{1 + \varepsilon}} - \frac{\sqrt{1 + \varepsilon}}{\lambda_{eq}}\right) + \frac{kT}{v}\left[\log\left(1 - \frac{1}{\lambda_{eq}^3}\right) + \frac{1}{\lambda_{eq}^3} + \frac{\chi}{\lambda_{eq}^6}\right] - \frac{\mu}{v}. \qquad (10)
\end{aligned}$$

It should be noticed that right after the stress is imposed on a fully swollen gel, at short-time limit, as the solvent inside the gel has no time to migrate to maintain the balance with the solvent outside, the chemical potential of the solvent inside the gel is not vanishing anymore, i.e., $\mu \neq 0$. For tensile stress, the gel tends to absorb more solvent so that the chemical potential of the solvent inside the gel decreases, $\mu < 0$. For compressive stress, the gel tends to expel solvent, which increases the chemical potential of the solvent inside the gel, $\mu > 0$. Under an uniaxial stress in N_1-direction, $\sigma_2 = \sigma_3 = 0$. By combining Eqs. (9) and (10), the stress σ_1 is given by

$$\sigma_1 = \frac{NkT}{\lambda_{eq}}\left[(1 + \varepsilon)^2 - \frac{1}{1 + \varepsilon}\right]. \tag{11}$$

This is a nonlinear stress–strain relation for a fully swollen gel under uniaxial stress state.

The linearized stress–strain relation is obtained by taking the leading term of strain ε, given by

$$\sigma_1 = \frac{3NkT\varepsilon}{\lambda_{\text{eq}}}. \tag{12}$$

The prefactor here is the elastic modulus at the short-time limit for infinitesimal strain,

$$E_{t=0^+}|_{\varepsilon=0} = \frac{3NkT}{\lambda_{\text{eq}}}. \tag{13}$$

At the short-time limit, as the solvent has no time to migrate out, the gel is considered incompressible, or equivalently, Poisson's ratio at the short-time limit for infinitesimal strain is

$$\nu_{t=0^+}|_{\varepsilon=0} = \frac{1}{2}. \tag{14}$$

Thus the shear modulus at the short-time limit for infinitesimal strain is

$$G_{t=0^+}|_{\varepsilon=0} = \frac{NkT}{\lambda_{\text{eq}}}. \tag{15}$$

At the short-time limit for infinitesimal strain, the shear modulus is the shear modulus NkT of the gel at the dry state divided by the equilibrium swelling ratio λ_{eq}. This extremely simple relation suggests a means to correlate the shear modulus of dry and fully swollen gel by the equilibrium swelling ratio.

In order to evaluate the linearized stress–strain relation (Eq. (12)), the comparison between the linear and nonlinear stress–strain relation (Eq. (11)) is shown in Fig. 3 where the normalized stress $\sigma_1 v/kT$ is plotted against nominal strain ε for different materials parameters and corresponding equilibrium swelling ratio λ_{eq}, namely ($Nv = 0.001$, $\chi = 0.2$, $\lambda_{\text{eq}} = 3.215$), ($Nv = 0.01$, $\chi = 0.2$, $\lambda_{\text{eq}} = 2.125$), and ($Nv = 0.05$, $\chi = 0.4$, $\lambda_{\text{eq}} = 1.513$). Here Nv is the normalized shear modulus of the dry polymer. It is found that the linearized stress–strain relation agrees very well with the nonlinear relation for a very wide range of strain, from –20% to +30%. It is interesting to find that the gels with relatively smaller equilibrium swelling ratios (e.g., $\lambda_{\text{eq}} = 1.513$) show more significant nonlinearity compared with the ones with larger equilibrium swelling ratios (e.g., $\lambda_{\text{eq}} = 3.215$). In fact, the gel with $\lambda_{\text{eq}} = 3.215$ shows almost linear stress–strain behavior as strain varies from –50% to 50%. The reason is that the nonlinearity is modulated by a prefactor in Eq. (11), NkT/λ_{eq}, and this prefactor dims for smaller shear modulus of dry polymer NkT and larger equilibrium swelling ratios λ_{eq}, which provides approximately linear stress–strain relation. In fact, these two factors, NkT and λ_{eq} change out-of-phase, e.g., smaller NkT corresponds to larger λ_{eq}, which makes the modulation effect of this prefactor NkT/λ_{eq} on the linearity of the stress–strain relation more pronounced. Thus Fig. 3 shows that the linearized stress–strain relation (such as the poroelasticity model Eq. (3)) with moduli given by Eqs. (13) and (15) is applicable to a reasonably large strain at the short-time limit.

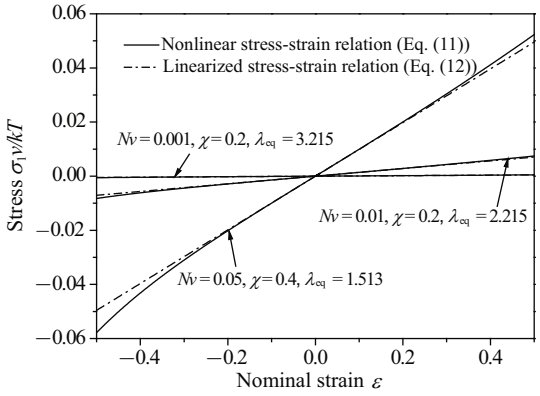

Fig. 3 Normalized stress $\sigma_1 v/kT$ versus nominal strain ε of a fully swollen gel subjected to uniaxial tension for both nonlinear constitutive and linearized constitutive relations at short-time limit. Three material parameters and corresponding swelling ratio are used, namely ($Nv = 0.001$, $\chi = 0.2$, $\lambda_{\text{eq}} = 3.215$), ($Nv = 0.01$, $\chi = 0.2$, $\lambda_{\text{eq}} = 2.125$), and ($Nv = 0.05$, $\chi = 0.4$, $\lambda_{\text{eq}} = 1.513$)

(2) Long-time limit: relaxed state

At the long-time limit, the new equilibrium state is reached. As the solvent inside the gel is able to migrate out to establish a balance with the solvent outside, the volume of the gel changes and the chemical potential of the solvent inside the gel is everywhere uniform and vanishing, i.e., $\mu = 0$, remaining balanced with the solvent outside.

Upon the uniaxial stress in N_1-direction, the nominal strain ε in N_1-direction is defined as the same way in Eq. (7). The Poisson's ratio at the long-time limit $t = \infty$ is introduced to relate the strain in N_1-direction and N_2-, N_3-directions,

$$\lambda_2 = \lambda_3 = \lambda_{\text{eq}}(1 - \nu_{t=\infty}\varepsilon). \tag{16}$$

The true stresses (Eq. (4)) are thus given by

$$\begin{aligned}\sigma_1 &= \frac{NkT}{\lambda_{\text{eq}}^2(1-\nu_{t=\infty}\varepsilon)^2}\left[\lambda_{\text{eq}}(1+\varepsilon) - \frac{1}{\lambda_{\text{eq}}(1+\varepsilon)}\right] \\ &\quad + \frac{kT}{v}\left\{\log\left[1 - \frac{1}{\lambda_{\text{eq}}^3(1+\varepsilon)(1-\nu_{t=\infty}\varepsilon)^2}\right]\right. \\ &\quad + \frac{1}{\lambda_{\text{eq}}^3(1+\varepsilon)(1-\nu_{t=\infty}\varepsilon)^2} \\ &\quad \left. + \frac{\chi}{\lambda_{\text{eq}}^6(1+\varepsilon)^2(1-\nu_{t=\infty}\varepsilon)^4}\right\}, \\ \sigma_2 &= \sigma_3 \\ &= \frac{NkT}{\lambda_{\text{eq}}^2(1+\varepsilon)(1-\nu_{t=\infty}\varepsilon)}\end{aligned} \tag{17}$$

$$\times \left[\lambda_{\mathrm{eq}}\left(1-\nu_{t=\infty}\varepsilon\right)-\frac{1}{\lambda_{\mathrm{eq}}\left(1-\nu_{t=\infty}\varepsilon\right)}\right]$$
$$+\frac{kT}{v}\left\{\log\left[1-\frac{1}{\lambda_{\mathrm{eq}}^3(1+\varepsilon)(1-\nu_{t=\infty}\varepsilon)^2}\right]\right.$$
$$+\frac{1}{\lambda_{\mathrm{eq}}^3(1+\varepsilon)(1-\nu_{t=\infty}\varepsilon)^2}$$
$$\left.+\frac{\chi}{\lambda_{\mathrm{eq}}^6(1+\varepsilon)^2(1-\nu_{t=\infty}\varepsilon)^4}\right\}, \tag{18}$$

This is the nonlinear stress–strain relation at the long-time limit. Using the traction free condition in N_2 and N_3 directions (i.e., $\sigma_2 = \sigma_3 = 0$), Poisson's ratio $\nu_{t=\infty}$ can be solved from Eq. (18). It is noticed that $\nu_{t=\infty}$ depends on strain ε. Substituting $\nu_{t=\infty}$ into Eq. (17), stress σ_1 can be expressed as a function of strain ε and two material parameters NkT and χ, along with Poisson's ratio $\nu_{t=\infty}$,

$$\sigma_1 = \frac{NkT}{\lambda_{\mathrm{eq}}}\left[\frac{1+\varepsilon}{\left(1-\nu_{t=\infty}\varepsilon\right)^2}-\frac{1}{1+\varepsilon}\right]. \tag{19}$$

This is the nonlinear stress–strain relation for the long-time limit. Because the presence of strain-dependent $\nu_{t=\infty}$, this stress–strain relation is not explicit.

Linearized relation is obtained by taking the leading term of ε. $\sigma_2 = 0$ and Eq. (18) give Poisson's ratio

$$\nu_{t=\infty}|_{\varepsilon=0} = \frac{1}{2}-\frac{Nv/\lambda_{\mathrm{eq}}}{2Nv/\lambda_{\mathrm{eq}}^3+2/(\lambda_{\mathrm{eq}}^3-1)-2/\lambda_{\mathrm{eq}}^3-4\chi/\lambda_{\mathrm{eq}}^6}. \tag{20}$$

Figure 4a shows the Poisson ratio $\nu_{t=\infty}$ as a function of strain ε, for different materials parameters and corresponding equilibrium swelling ratio λ_{eq}, namely ($Nv = 0.001$, $\chi = 0.2$, $\lambda_{\mathrm{eq}} = 3.215$), ($Nv = 0.01$, $\chi = 0.2$, $\lambda_{\mathrm{eq}} = 2.125$), and ($Nv = 0.05$, $\chi = 0.4$, $\lambda_{\mathrm{eq}} = 1.513$). The approximated Poisson's ratios for the infinitesimal strain are marked as $*$ in each curve. The results show that Poisson's ratio has strain dependence, but not very strong as for a fairly wide range of strain (from –10% to 10%), Poisson's ratios varies slightly. Secondly, it is also observed that Poisson's ratios are around 0.25 for these three materials properties. Therefore, Poisson's ratio of the gel at the long-time limit can be approximately considered as strain independent and given by Eq. (20).

Given that Poisson's ratio $\nu_{t=\infty}$ can be considered as strain independent, the nonlinear stress–strain relation at the long-time limit (Eq. (17)) can be linearized by taking the linear term of strain ε, which gives a very simple relation,

$$\sigma_1 = \frac{2NkT\left(1+\nu_\infty\right)\varepsilon}{\lambda_{\mathrm{eq}}}. \tag{21}$$

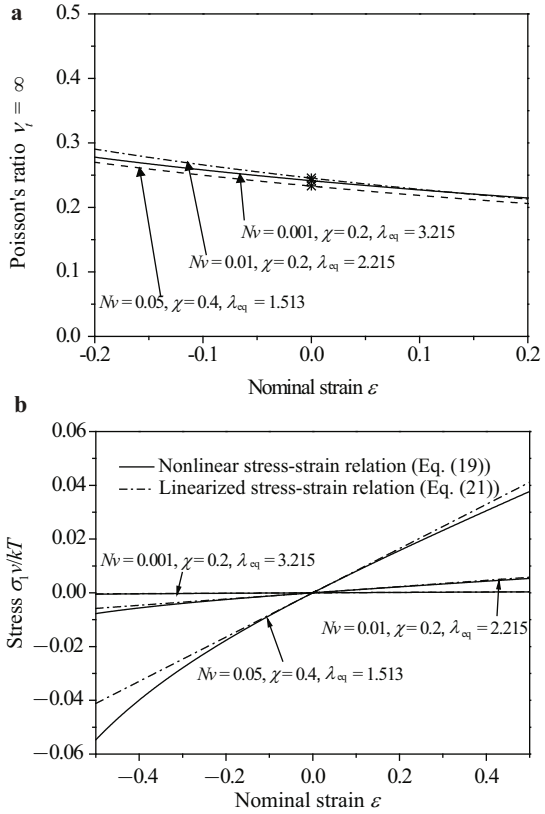

Fig. 4 A fully swollen gel subjected to uniaxial tension for both nonlinear constitutive and linearized constitutive relations at long-time limit. **a** Poisson's ratio $\nu_{t=\infty}$ versus nominal strain ε, where "*" denotes the linearized value; **b** Normalized stress $\sigma_1 v/kT$ versus nominal strain ε. Three material parameters and corresponding swelling ratio are used, namely ($Nv = 0.001, \chi = 0.2, \lambda_{\mathrm{eq}} = 3.215$), ($Nv = 0.01, \chi = 0.2, \lambda_{\mathrm{eq}} = 2.125$), and ($Nv = 0.05, \chi = 0.4, \lambda_{\mathrm{eq}} = 1.513$)

The prefactor defines the elastic modulus at the long-time limit for infinitesimal strain,

$$E_{t=\infty}|_{\varepsilon=0} = \frac{2NkT\left(1+\nu_\infty\right)}{\lambda_{\mathrm{eq}}}. \tag{22}$$

Recalling Eq. (13), the relation between the elastic moduli at the short-time limit and long-time limit for infinitesimal strain is given by

$$E_{t=\infty}|_{\varepsilon=0} = E_{t=0^+}|_{\varepsilon=0}\,\frac{2\left(1+\nu_\infty\right)}{3}. \tag{23}$$

As $\nu_\infty < 1/2$, $E_{t=\infty}|_{\varepsilon=0} < E_{t=0^+}|_{\varepsilon=0}$, which indicates as time evolves the solvent migrates out of the gel and the gel becomes softer. More surprisingly, the shear modulus at the long-time limit

$$G_{t=\infty}|_{\varepsilon=0} = \frac{E_{t=\infty}|_{\varepsilon=0}}{2\left(1+\nu_\infty\right)} = G_{t=0^+}|_{\varepsilon=0} = \frac{NkT}{\lambda_{\mathrm{eq}}}, \tag{24}$$

by using Eq. (15). The same shear modulus at the short-time and long-time limits is because the difference for these

two limits lies on the volumetric compressibility, i.e., incompressible at the short-time limit and compressible at the long-time limit. However, the shear modulus characterizes the relation between shear stress and shear strain, which does not induce volumetric change. Therefore, the shear moduli at the short-time and long-time limits are the same.

Figure 4b shows the normalized stress $\sigma_1 v/kT$ as a function of nominal strain ε for both nonlinear relation (Eq. (19)) and linearized relation (Eq. (21)) for different materials parameters and equilibrium swelling ratio λ_{eq}, namely (Nv = 0.001, χ = 0.2, λ_{eq} = 3.215), (Nv = 0.01, χ = 0.2, λ_{eq} = 2.125), and (Nv = 0.05, χ = 0.4, λ_{eq} = 1.513). Similarly to Fig. 3 for short-time limit, the nonlinear and linearized stress–strain relations agree very well for a very wide range of strain, from –20% to +30%. The gel with larger equilibrium swelling ratio also shows better linearity compared with that with smaller equilibrium swelling ratio. Thus Fig. 4b shows that the linearized stress–strain relation is a good approximation to the nonlinear stress–strain relation, even for a reasonably large strain at the long-time limit.

The studies in this section conclude that the fully swollen gel behaves pronounced linear stress–strain relation for a significant range of strain. Therefore, the porelasticity model can capture the stress–strain behavior of fully swollen gel even for large strain. The moduli for short-time and long-time limits depend on the modulus of the dry polymer and the swelling ratio.

3 Finite element analysis of gel indentation with large deformation effect

Figure 2 has shown that the large deformation plays a critical role on indentation for hard materials. In this section, we will examine this effect by indenting a fully swollen gel that presents good linear stress–strain behavior as shown in Sect. 2. The finite element analysis is conducted in ABAQUS and the two extreme cases, namely, short-time and long-time limits, are discussed separately. The constitutive relation of gels is implemented in ABAQUS via its user-defined hyperelastic material (UHYPER) [22].

3.1 Short-time limit: a transient analysis

At short-time limit upon a fully swollen gel subjected load, the solvent has no time to migrate so that the balance between the solvent inside and outside the gel is broken. The chemical potential of the solvent inside the gel thus instantaneously deviates from its initial value (μ = 0) at the fully swollen state and the deviation depends on the specific load. Therefore, the chemical potential of the solvent inside the gel is a field variable as the stress and strain of the gel are nonuniform upon indentation. This is a transient problem of coupled deformation and diffusion. Zhang et al. [23] has developed a user element in ABAQUS to study this coupled problem to treat displacement and chemical potential as independent field variables. An alternative way is to utilize the analogy between diffusion and heat transfer as they are all transport problem with similar governing equations. An approach to implement this analogy in ABAQUS has developed using a user-defined heat transfer subroutine (UMATHT) in which the chemical potential is analogous to temperature and the coupled displacement and thermal elements in ABAQUS can be used to study the coupled displacement and diffusion. The evolution of temperature is thus equivalent to that of chemical potential of solvent.

At the short-time limit, the fully swollen gel is incompressible. For large deformation, this incompressibility condition requires

$$\det(\boldsymbol{F}) = \lambda_{eq}^3, \tag{25}$$

where $\boldsymbol{F}$ is the deformation gradient with the dry state as the reference state. To implement this condition, a penalty function is added to the subroutine UHYPER.

It should be noticed that this transient analysis should be rigorously evaluated at vanishing time, i.e., $t \to 0^+$, which impose difficulty on the numerical implementation. Meanwhile, this transient analysis is also subjected to the incompressible constraint, which actually is an effective requirement for short-time limit as the gel is compressible right after $t > 0$. For the sake of simplicity of numerical implementation, we use relatively large time and the incompressible condition in the simulations for short-time limit and we find this treatment is very accurate. To benchmark this implementation, we study the uniaxial tension of a fully swollen gel using 640 three-dimensional coupled displacement-temperature elements (C3D8T elements in ABAQUS) and the finite element results totally collapse with the stress–strain relation given by Eq. (11) as shown in Fig. 5. The material parameters are $Nv = 0.001, \chi = 0.2$, and the corresponding equilibrium swelling ratio $\lambda_{eq} = 3.215$.

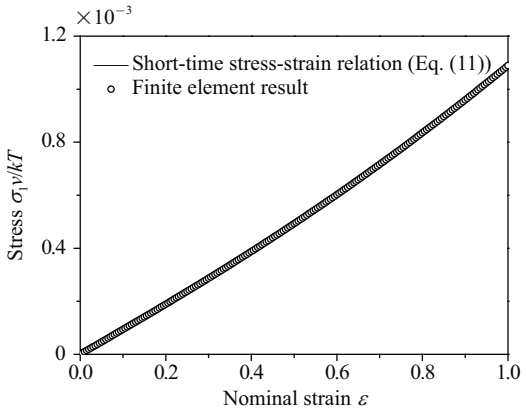

Fig. 5 Normalized stress $\sigma_1 v/kT$ versus nominal strain ε of a fully swollen gel subjected to uniaxial tension at the short-time limit, obtained by both finite element analysis and analytical results. The material parameters are $Nv = 0.001, \chi = 0.2, \lambda_{eq} = 3.215$

The gel indentation is then studied using this approach. A spherical indenter with radius R = 9 mm is modeled as a

rigid and impermeable material. A fully swelling gel is modeled by 12 395 C3D8T elements. To capture the localized deformation in the gel, around 400 elements are used underneath the indenter. The contact between indenter and gel is considered frictionless. Both nonlinear and linearized constitutive relations are used to characterize the gel. As the deformation is three-dimensional, the nonlinear constitutive relation is described by the UHYPER subroutine, which equivalently gives Eq. (4). To compare with the linearized model, the porelasticity model (Eq. (3)) is also used with the shear modulus G given by Eq. (15) and Poisson's ratio $\nu = 0.5$. Figure 6a shows the indentation force F versus indentation depth h for both nonlinear and linearized stress–strain relations with material parameters $Nv = 0.001$, $\chi = 0.2$, and the corresponding equilibrium swelling ratio $\lambda_{\text{eq}} = 3.215$. There is distinguishable difference between nonlinear and linearized constitutive relations when the indentation depth approximately exceeds 1 mm, though this discrepancy is minor.

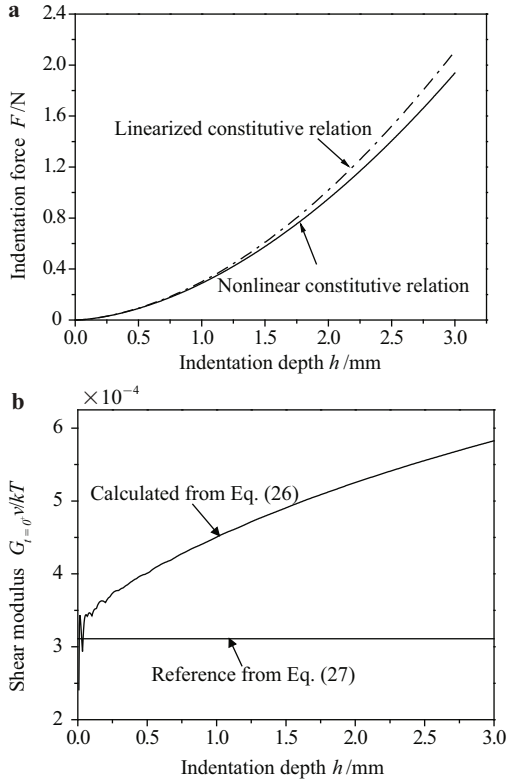

Fig. 6 Indenting a fully swollen gel with normalized shear modulus $Nv = 0.001$ and the solvent-polymer interaction parameter $\chi = 0.2$ by a rigid spherical indenter with radius of 9 mm at the short-time limit using finite element analysis. **a** Indentation force F versus indentation depth h; **b** Shear modulus $G_{t=0^+}v/kT$ versus indentation depth h

A more important evaluation is if the indentation force can be used to calculate the shear modulus of the gel. Given that the fully swollen gel is incompressible at the short-time limit (i.e., $\nu_{t=0^+}|_{\varepsilon=0} = 1/2$), the indentation force F for a spherical indenter with radius R and indentation depth h is given by Eqs. (1) and (2),

$$F(0) = \frac{16GR^{1/2}h^{3/2}}{3}. \tag{26}$$

Thus by knowing $F(0)$ and h for given R, the shear modulus of a fully swollen gel can be calculated. Based on Eq. (15), the normalized shear modulus of a fully swollen gel is

$$\frac{G_{t=0^+}|_{\varepsilon=0}\, v}{kT} = \frac{Nv}{\lambda_{\text{eq}}}, \tag{27}$$

where $Nv = 0.001$ and $\lambda_{\text{eq}} = 3.215$ in this finite element analysis. Equation (27) provides a reference as the benchmark for the shear modulus obtained from Eq. (26).

Figure 6b compares the shear modulus of the fully swollen gel calculated from the indentation force $F(0)$ (Eq. (26)) and the reference given by Eq. (27). As the indentation is shallow (i.e., very small h), the calculated shear modulus is consistent with the reference value, though there are some oscillations, which is caused by the numerical errors (or equivalently experimental errors) for very shallow indentations. This consistency indicates that the indentation experiment does provide a way to calculate the shear modulus of a fully swollen gel. When the indentation depth h increases, the oscillation becomes smaller; however, the calculated shear modulus starts to significantly deviate from the reference. Large deformation again makes Eq. (26) (or equivalently Eq. (2)) invalid as the hard materials do. In order to resolve this deviation or the effect of large deformation and keep using the simply equation as Eq. (2), empirical corrections have been applied [14]. These correction functions are helpful to calculate the shear modulus from the measured indentation force for large deformation but they are material specific. The advantage of the simply indentation experiments is somewhat mitigated.

These studies show that at the short-time limit, the indentation experiment do not provide a robust approach to measure the shear modulus of the fully swollen gel. If the indentation depth is very small, Eq. (26) (or equivalently Eq. (2)) is valid. However, the noise from such a small deformation makes the results oscillation, which provides another uncertainty for the measurement. If the indentation depth is large, the relation between indentation depth and shear modulus is not valid any longer.

3.2 Long-time limit: a static analysis

At long-time limit, solvent has sufficient time to migrate in and out of the gel and a new equilibrium state is reached. Solvent inside balances with solvent outside, characterized by an uniform chemical potential $\mu = 0$ everywhere inside the gel. It is thus a steady state problem, in which the chemical potential is just a parameter but a field variable. Therefore, the active degree of freedom is just displacement. The stress–strain relation is implemented via UHYPER in

ABAQUS. A similar benchmark is conducted by studying an uniaxial tension of a fully swollen gel, similar to that for the short-time limit. 640 three-dimensional displacement elements (C3D8 elements in ABAQUS) are used. Figure 7 shows that the finite element results completely agree with the stress–strain relation given by Eq. (21). The material parameters are $Nv = 0.001$, $\chi = 0.2$, and the corresponding equilibrium swelling ratio $\lambda_{eq} = 3.215$.

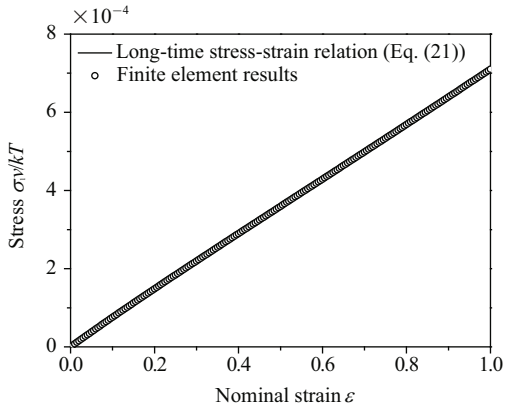

Fig. 7 Normalized stress $\sigma_1 v/kT$ versus nominal strain ε of a fully swollen gel subjected to uniaxial tension at the long-time limit, obtained by both finite element analysis and analytical results. The material parameters are $Nv = 0.001, \chi = 0.2, \lambda_{eq} = 3.215$

For long-time limit experiment, the main interest is to measure the Poisson's ratio. Given that the shear moduli are the same for short-time and long-time limits and a fully swollen gel is incompressible at the short-time limit, Eq. (2) gives a ratio between indentation forces at the short-time (i.e., $F(0)$) and at the long-time limit (i.e., $F(\infty)$),

$$\frac{F(0)}{F(\infty)} = 2(1 - \nu_{t=\infty}). \tag{28}$$

Using Eq. (28), the Poisson's ratio is calculated as a function of the indentation depth h as shown in Fig. 8a. Here only the nonlinear stress–strain relation (i.e., Eq. (4)) is used. The material parameters are $Nv = 0.001$, $\chi = 0.2$, and the corresponding equilibrium swelling ratio $\lambda_{eq} = 3.215$. At smaller indentation depth, the Poisson's ratio is about 0.28, which is within the range of Poisson's ratio presented in Fig. 4a. Therefore, the ratio in Eq. (28) can be used to measure the Poisson's ratio, though the oscillation is apparent for very small strain. However, as the increase of the indentation depth, the Poisson's ratio increases and shows a fairly strong dependence on the indentation depth. The reason is that intrinsic dependence on strain of Poisson's ratio at long-time limit (Eq. (18)) becomes more pronounced for large strains where usually occur underneath the indenter. Figure 8b illustrates the strain contour for $h = 1.5$ mm, where the maximum strain underneath the indenter exceeds 30% but the smaller strain in the gel is only 2%.

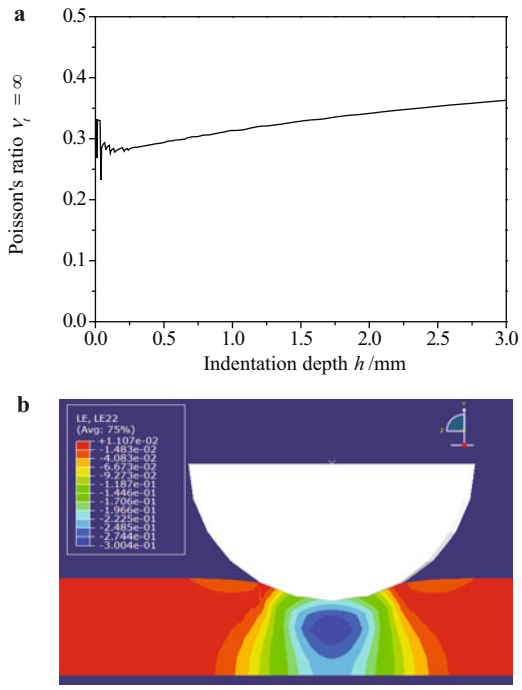

Fig. 8 Indenting a fully swollen gel with normalized shear modulus $Nv = 0.001$ and the solvent-polymer interaction parameter $\chi = 0.2$ by a rigid spherical indenter with radius of 9 mm at the long-time limit using finite element analysis. **a** Poisson's ratio $\nu_{t=\infty}$ versus indentation depth h; **b** strain contour for $h = 1.5$ mm

This study shows that as the Poisson's ratio is strain dependent as shown in Fig. 4a and indentation leads to very non-uniform strain state, the Poisson's ratio calculated from the ratio between the indentation forces at the short-time and long-time limits has a fairly strong dependence on the strain and can not be considered as a material property.

4 Proposed experiment: uniaxial compression

The limitations of the indentation on gels mainly are resulted from two factors, (1) the basic equation to relate the indentation force and indentation depth is usually for infinitesimal deformation (e.g., Eq. (2) for spherical indenter) and its counterpart for large deformation has no explicitly analytical expression, and (2) the strain state is non-uniform. To overcome these limitations, an uniaxial compression experiment is proposed as shown in Fig. 9, where a fully swollen gel in cylindrical shape is uniformly compressed by two impermeable plates. The interface is lubricated by hydrophobic materials to allow lateral deformation.

The size of the fully swollen gel is $\pi\left(R\lambda_{eq}\right)^2 \times H\lambda_{eq}$, where $\pi R^2 \times H$ is the size of the dry gel. At short-time limit, from Eqs. (7), (8) and (11), the applied force $F(0)$ and the nominal strain ε follows this relation

$$F(0) = NkT\lambda_{eq}\pi R^2\left[1 + \varepsilon - \frac{1}{(1+\varepsilon)^2}\right]. \tag{29}$$

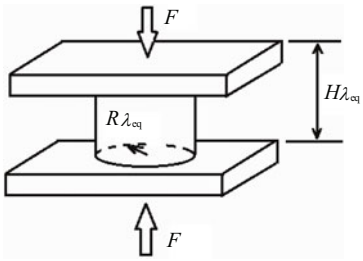

Fig. 9 Schematic of a fully swollen gel under uniaxial compression

At long-time limit, from Eqs. (16) and (19), the applied force $F(\infty)$ and the nominal strain ε follows this relation

$$F(\infty) = NkT\lambda_{\text{eq}}\pi R^2\left[1+\varepsilon-\frac{(1-\nu_{t=\infty}\varepsilon)^2}{1+\varepsilon}\right]. \tag{30}$$

The two curves, $F(0)$ vs. ε and $F(\infty)$ vs. ε, are able to calculate NkT and $\nu_{t=\infty}$.

5 Concluding remarks

In this paper, we have conducted both analytical modeling and finite element analysis to evaluate the effects of large deformation and material nonlinearity on gel indentation experiment. Specifically, we have analyzed if the basis of indentation, namely relation between the indentation force and indentation depth with the prefactor related to the modulus of indented material, can be accurately applied to gel in which the deformation is large and the material behavior is nonlinear. The analytical modeling is based on a coupled large deformation and mass diffusion model and the finite element analysis uses two user-defined subroutines, UMATHT and UHYPER, in finite element package ABAQUS. It is found that large deformation significantly deviates the relation between indentation force and indentation depth from that for small deformation. Thus, the classical relation between indentation force and depth can be only applied to very shallow indentation, which extremely limits the application to the gel indentation since the gel is soft and the deformation is usually large. This paper also found that the material nonlinearity does not play a very important role on indentation experiment so that the poroelasticity that has been used in many existing studies is a good approximation. Based on these observations, this paper also proposes an alternative approach to measure the mechanical properties of gels, namely, uniaxial compression experiment. The proposed approach can be applied to both small and large deformation and the material nonlinearity has been included. Besides the large deformation and the material nonlinearity effects that are studied in this paper, the size effects of the contact region and the indent material are also expected to be important to evaluate the indentation experiment, which is a separate topic to be studied.

Acknowledgement We appreciate the High Performance Computing Initiative (HPCI) at the Arizona State University. YA acknowledges the financial support from the China Scholarship Council.

References

1 Duncan, R.: The dawning era of polymer therapeutics. Nature Reviews Drug Discovery **2**, 347–360 (2003)

2 Peppas, N. A., Hilt, J. Z., Khademhosseini, A., et al.: Hydrogels in biology and medicine: From molecular principles to bionanotechnology. Advanced Materials **18**, 1345–1360 (2006)

3 Lee, K. Y., Mooney, D. J.: Hydrogels for tissue engineering. Chemical Reviews **101**, 1869–1879 (2001)

4 Varghese, S., Elisseeff, J. H.: Hydrogels for musculoskeletal tissue engineering. Polymers for Regenerative Medicine. (2006). DOI: 10.1007/12-072

5 Zhang, J. H., Daubert, C. R., Foegeding, E. A.: Fracture analysis of alginate gels. Journal of Food Science **70**, E425–E431 (2005)

6 Cai, S. Q., Lou, Y. C., Ganguly, P., et al.: Force generated by a swelling elastomer subject to constraint. Journal of Applied Physics **107**, (2010)

7 John, G., Jadhav, S. R., Hong, E.: Phase-selective molecular gels: A new tool for recovery of an oil from oil spills/petroleum products. Abstracts of Papers of the American Chemical Society **241**, 18–28 (2011)

8 Ebenstein, D. M., Pruitt, L. A.: Nanoindentation of soft hydrated materials for application to vascular tissues. Journal of Biomedical Materials Research Part A **69A**, 222–232 (2004)

9 Kaufman, J. D., Miller, G. J., Morgan, E. F., et al.: Time-dependent mechanical characterization of poly(2-hydroxyethyl methacrylate) hydrogels using nanoindentation and unconfined compression. Journal of Materials Research **23**, 1472–1481 (2008)

10 Lake, S. P., Hald, E. S., Barocas, V. H.: Collagen-agarose cogels as a model for collagen-matrix interaction in soft tissues subjected to indentation. Journal of Biomedical Materials Research Part A **99A**, 507–515 (2011)

11 Kalcioglu, Z. I., Mahmoodian, R., Hu, Y. H., et al.: From macro- to microscale poroelastic characterization of polymeric hydrogels via indentation. Soft Matter **8**, 3393–3398 (2012)

12 Hu, Y. H., Zhao, X. H., Vlassak, J. J., et al.: Using indentation to characterize the poroelasticity of gels. Applied Physics Letters **96**, 121904 (2010)

13 Cai, S. Q., Hu, Y. H., Zhao, X. H., et al.: Poroelasticity of a covalently crosslinked alginate hydrogel under compression. Journal of Applied Physics **108**, 113514 (2010)

14 Hu, Y. H., Chan, E. P., Vlassak, J. J., et al.: Poroelastic relaxation indentation of thin layers of gels. Journal of Applied Physics **110**, 086103 (2011)

15 Chan, E. P., Hu, Y. H., Johnson, P. M., et al.: Spherical indentation testing of poroelastic relaxations in thin hydrogel layers. Soft Matter **8**, 1492–1498 (2012)

16 Long, R., Hall, M. S., Wu, M. M., et al.: Effects of gel thickness on microscopic indentation measurements of gel modulus. Biophysical Journal **101**, 643–650 (2011)

17 Quinn, T. M., Grodzinsky, A. J.: Longitudinal modulus and hy-

draulic permeability of poly(methacrylic acid) gels - effects of charge-density and solvent content. Macromolecules **26**, 4332–4338 (1993)

18 Yu, H. Y., Sanday, S. C., Rath, B. B.: The effect of substrate on the elastic properties of films determined by the indentation test - axisymmetrical boussinesq problem. Journal of the Mechanics and Physics of Solids **38**, 745–764 (1990)

19 Hong, W., Zhao, X. H., Zhou, J. X., et al.: A theory of coupled diffusion and large deformation in polymeric gels. Journal of the Mechanics and Physics of Solids **56**, 1779–1793 (2008)

20 Galli, M., Oyen, M. L.: Fast identification of poroelastic parameters from indentation tests. Cmes-Computer Modeling in Engineering & Sciences **48**, 241–269 (2009)

21 Galli, M., Comley, K. S. C., Shean, T. A. V., et al.: Viscoelastic and poroelastic mechanical characterization of hydrated gels. Journal of Materials Research **24**, 973–979 (2009)

22 Hong, W., Liu, Z. S., Suo, Z. G.: Inhomogeneous swelling of a gel in equilibrium with a solvent and mechanical load. International Journal of Solids and Structures **46**, 3282–3289 (2009)

23 Zhang, J. P., Zhao, X. H., Suo, Z. G., et al.: A finite element method for transient analysis of concurrent large deformation and mass transport in gels. Journal of Applied Physics **105**, 093522 (2009)